IOPscience iopscience.iop.org

Home Search Collections Journals About Contact us My IOPscience

Growth dynamics of insulating SrF_2 films on Si(111)

This article has been downloaded from IOPscience. Please scroll down to see the full text article.

2007 J. Phys.: Condens. Matter 19 445001

(http://iopscience.iop.org/0953-8984/19/44/445001)

View the table of contents for this issue, or go to the journal homepage for more

Download details:
IP Address: 129.252.86.83
The article was downloaded on 29/05/2010 at 06:28

Please note that terms and conditions apply.

IOP PUBLISHING JOURNAL OF PHYSICS: CONDENSED MATTER

J. Phys.: Condens. Matter **19** (2007) 445001 (9pp) doi:10.1088/0953-8984/19/44/445001

Growth dynamics of insulating SrF_2 films on Si(111)

Y Seino[1], **S Yoshikawa**[1], **M Abe**[1,2] **and S Morita**[1]

[1] Graduate School of Engineering, Osaka University, 2-1 Yamada-oka, Suita, Osaka 565-0871, Japan
[2] PRESTO, Japan Science and Technology Agency, Saitama 332-0012, Japan

E-mail: seino@eei.eng.osaka-u.ac.jp

Received 31 January 2007, in final form 30 April 2007
Published 18 October 2007
Online at stacks.iop.org/JPhysCM/19/445001

Abstract
Most high-resolution scanning tunnelling microscopy studies on insulating films thus far have been restricted to samples of less than one monolayer thickness on conducting substrates. On the other hand, insulating films with more than one monolayer are crucial to electrically decouple the conducting substrate. In such a case, atomic force microscopy is required to explore the growth dynamics of the insulating films. In this paper, we discuss the growth dynamics of an insulating SrF_2 film surface on an Si(111) substrate imaged by non-contact atomic force microscopy (NC-AFM) at room temperature in ultrahigh vacuum. For ∼0.7 monolayer SrF_2 coverage, the coexisting surfaces of the SrF_2 row structure and Si(111)-(7×7) reconstruction are clearly observed by NC-AFM topography measurements, indicating evidence for reactive Si dangling bonds at the outermost tip apex. We also discuss the tip character obtained from two types of topographic images. In addition, we determined that the conformation changes from the row structure to (1×1) periodicity by further SrF_2 evaporation.

(Some figures in this article are in colour only in the electronic version)

1. Introduction

Insulating films are crucial for electrical isolation in electronic devices. The operation of such devices should be governed by the electrical properties and structures, and certain isolation between functional elemental devices plays a significant role for enhanced performance even when the separation approaches the atomic scale. Furthermore, when the thickness of the insulating films thins more and more, the composite phenomena will appear progressively in conjunction with the surface and interface effects, which are influenced by a wide variety of effects, including the electronic structure of the substrate, the insulator film, and/or interface between them, band-bending effects induced by the electric field between the tip and the sample, field resonances, image potential states, and the local work function.

© 2007 IOP Publishing Ltd Printed in the UK

Table 1. Silicon and fluoride material parameters. Lattice constants at room temperature and growth temperature, and their ratios to those of the Si substrate and energy gaps [17].

Materials	Lattice constant 298 K (nm)	Ratio to Si	Lattice constant 1005 K (nm)	Ratio to Si	Energy gap (eV)
Si	0.5431	1.000	0.5440	1.000	1.1
CaF_2	0.5463	1.006	0.5571	1.024	12.1
SrF_2	0.5799	1.068	0.5880	1.081	11.3
BaF_2	0.6200	1.142	0.6305	1.159	11.0

While scanning tunnelling microscopy (STM) is an established technique to analyse the surface structures of conducting surfaces by real-space imaging, the quality of the image strongly depends on the substrate conductivity. Atomic force microscopy (AFM) is a unique method to reveal the growth dynamics of insulating materials by high-resolution imaging. Indeed, the recent development of non-contact AFM (NC-AFM) [1] has opened up the possibility of measuring the topography of semiconducting [2–4], metallic [5] and insulating surfaces [6, 7] with true atomic resolution. This is very significant since NC-AFM observations can reveal the real surface structure at atomic scale of even insulating surfaces.

In contrast to STM, NC-AFM involves many different tip–sample interactions, each with a different length scale, resulting in a non-monotonic tip–sample distance dependence of the interaction. Although both short- and long-range interactions contribute to the tip–sample forces converted from the measured frequency shift, only short-range forces give atomic-scale information. Thus, combined analysis is needed to analyse the interpretation of actual NC-AFM experimental information.

The surfaces of highly homologous materials are most often applicable in atomic resolution imaging using the NC-AFM. In particular, atomic resolution imaging can be achieved on flat and homogeneous terraces. On the other hand, it is quite difficult to obtain images with atomic/molecular-scale resolution across step sites or on heterogeneous surfaces. There are nevertheless a few previous reports on observations of heterogeneous materials and structural non-homologous surfaces by atomic/molecular resolution NC-AFM, including alkali halides on metal substrates [8] and organic molecules on insulating substrates [9, 10].

As a candidate heterogeneous material and structural non-homologous surface, an epitaxial semiconductor–insulator system, alkali-earth fluorides on Si(111), is employed for NC-AFM imaging. The system is of intrinsic scientific interest as well as technologically important. The scientific interest arises from questions involving interface formation between dissimilar materials, ionic compound insulators such as calcium fluoride (CaF_2) and strontium fluoride (SrF_2), and covalent homopolar semiconductors such as Si and Ge. The technological interest lies in the development of crystalline dielectrics for use in novel integrated circuits [13] and potential applications in functional inorganic fluorine chemistry.

SrF_2 is chemically very similar to CaF_2, however, its lattice constant is significantly larger than that of CaF_2 (see table 1). Also, the SrF_2–Si lattice mismatch is 6.8% at room temperature and 8.1% at the optimal growth temperature. Photo-emission studies on ultrathin films have shown that the bonding and charge transfer in the first monolayer at the SrF_2/Si(111) interface is very similar to that at the CaF_2/Si(111) interface [17]. The interface consists of a non-stoichiometric Si–(Ca, Sr)–F layer with the interface bond derived from silicon and cation orbitals at the optimal growth temperature. The early stages of CaF_2 growth on Si(111) have been studied experimentally with the aim of determining the interface structure and the growth mechanism. The CaF_2/Si(111) interface structure for submonolayer coverage has been

characterized assuming that the F layer, which would be present at the interface for fully stoichiometric CaF_2, is missing, and that Ca atoms most likely reside in one of three high-symmetry sites on the Si(111) surface: directly above the top Si layer (top site), above the second Si layer (T_4 site), or above the fourth Si layer (H_3 site). In thicker films, the CaF_2 overlayers are found to be rotated 180° with respect to the underlying Si(111) substrate, the so-called 'type-B' epitaxy [14]. Fluoride films of high crystalline quality with the crystal axes rotated through 180° relative to the Si(111) substrate can be epitaxially grown for both CaF_2 and SrF_2 [15]. Theoretical studies of CaF_2/Si(111) indicate that the T_4 structure has the lowest total energy in various models [16].

In this paper, we discuss the growth dynamics of insulating SrF_2 films on Si(111) by NC-AFM and show the conformational changes due to the role of lattice mismatch by the amount of insulating SrF_2 evaporation. In addition, we also show novel NC-AFM results on a surface under 0.7 monolayer SrF_2 evaporation, and the results of a detailed study on structural conformation change between 0.4 and 2.2 monolayers evaporation.

2. Experiment

2.1. Sample preparation and force microscopy

All SrF_2 film surfaces were prepared on Si(111) substrates after cleaning the substrate by direct current heating in an ultrahigh vacuum (UHV) environment and obtaining the Si(111)-(7 × 7) surface. The SrF_2 films were evaporated at a substrate temperature of around 700° C with an evaporation rate of 0.1 monolayer (ML) per minute (1 ML = 7.84×10^{14} atoms cm^{-2}). The substrate temperature was determined on the basis of the SrF_2 growth condition so as ensure that fluorine was not removed from the surface [18, 19]. By adjusting the initial amount of SrF_2 evaporated on the Si(111)-(7 × 7) surface, the evaporation rate can be determined by the structural change between the SrF_2 row-like arrangement and the bulk (1 × 1) periodicity [18].

All experiments were performed using a dynamic scanning force microscope (SFM) in a UHV environment operated using the frequency modulation (FM) detection method [20] and constant oscillation amplitude of a cantilever. Dynamic SFM measures the change in the first mechanical resonant frequency (the frequency shift, Δf) of an oscillating cantilever due to the interaction of a tip at the end of the cantilever with the surface. Data acquisition was performed using a commercial scanning probe microscope controller (*Dulcinea*, Nanotec, S L, Madrid, Spain) [21]. Commercially obtained Si cantilevers (Nanoworld AG, Neuchatel, Switzerland) were cleaned in UHV by Ar ion sputtering. The system is equipped with an analogue FM demodulator in order to measure Δf. All images were recorded in the constant Δf mode, wherein the detuning was kept constant during scanning.

3. Results and discussion

3.1. ∼0.7 monolayer coverage of SrF_2 on Si(111)

In the case of CaF_2 growth on Si(111), two-dimensional calcium monofluoride (CaF) islands were formed both at the step sites and the terraces, and had a (1 × 1) periodicity with respect to the Si(111) structure below 1 ML coverage [22–24]. In the SrF_2/Si(111) system, the surface structure under 0.7 ML deposition of SrF_2 (1 ML = 7.84×10^{14} atoms cm^{-2}) exhibits a multi-domain (5 × 1) LEED pattern due to large lattice mismatch [18]. Subsequent deposition, furthermore, promotes the F–Sr–F triple layer growth with each ion in a bulk-like

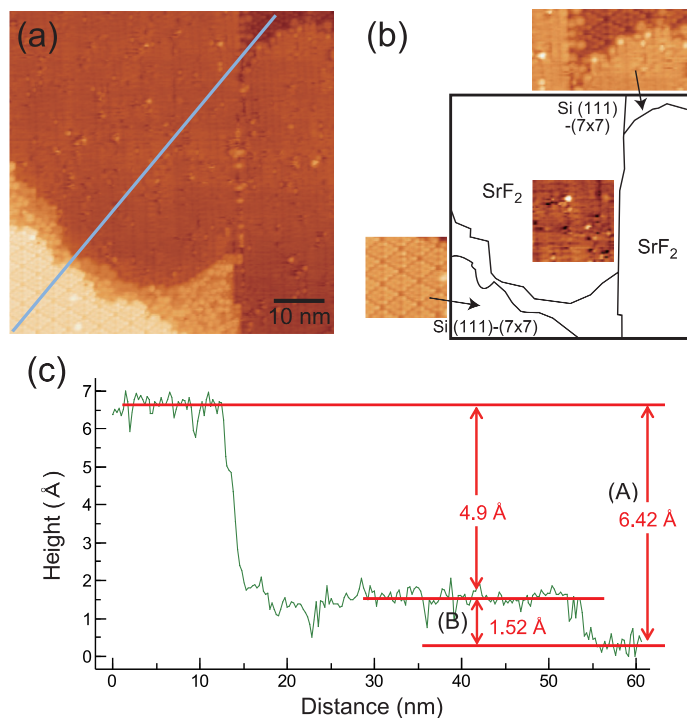

Figure 1. (a) NC-AFM topographic image on the surface of SrF_2/Si(111) with 0.4 ML SrF_2 coverage. The scanning size was 48 × 48 nm^2, (b) enlarged images of each terrace, and (c) cross-sectional profile of the solid line in (a). The acquisition parameters—the first mechanical resonant frequency (f_0), the oscillation amplitude (A) of the cantilever, and the Δf set point were $f_0 =$ 172 222.0 Hz, $A = 6$ nm, and $\Delta f = -19.6$ Hz respectively.

environment [18], and the surface structure exhibits the same features in comparison with the (1 × 1) hexagonal arrangement of the bulk.

Figures 1(a) and (b) show an NC-AFM topographic image on the surface of SrF_2/Si(111) with 0.4 ML coverage and the magnified image of each arrowed area by adjusting the appropriate image contrast, indicating the (7 × 7) surface structure, respectively. The topographic image in figure 1 provided us with the following information. The row structures of the SrF_2 and Si(111)-(7 × 7) reconstructed surface were observed simultaneously at the Si(111) terrace. This means that the topographic image was obtained using a Si dangling-bond tip apex. In NC-AFM, the good sharpness of the AFM tip is a prerequisite for obtaining high vertical and lateral contrast on heterogeneous surfaces [25]. The measured step height (A) in figure 1(c) corresponded to double steps of Si, and the quality of the topographic image was equivalent to that of the homogeneous Si(111)-(7 × 7) surface. Theoretical predictions indicate the possibility that using dangling-bond-terminated Si tips offers the opportunity for chemically resolved imaging of insulating surfaces due to stronger interactions with the surface anions [26]. This is, therefore, consistent with the notion that the row structures seen in the image are formed by the fluorine atoms or molecules[3].

[3] The dissipative image obtained by the type I tip apex in figure 2(b) was obtained simultaneously from the topographic image in figure 2(a). However, no dissipative image by the type II tip apex changed under scanning. This indicates that the topmost constituents could be fluorine compounds, whereas the corrugation of the topographic image in figure 2(c) represents strontium ions or its constituents by the simple structural assumptions from both images in figures 2(a) and (c).

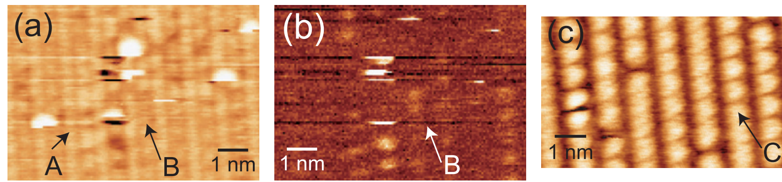

Figure 2. High resolution NC-AFM (a) topographic and (b) dissipative images obtained with a type I tip, and (c) high resolution topographic image obtained with a type II tip on the surface of $SrF_2/Si(111)$ for 0.4 ML SrF_2 coverage. (a) and (b) were obtained simultaneously with the type I tip. Scanning sizes are (a), (b) 8.3 × 5.8 nm^2 and (c) 8.0 × 4.8 nm^2, respectively. The acquisition parameters were (a), (b) $f_0 = 172\,222.0$ Hz, $A = 6$ nm, $\Delta f = -23.5$ Hz, and (c) $f_0 = 172\,203.0$ Hz, $A = 6$ nm, $\Delta f = -25.0$ Hz, respectively.

The rows on this surface were aligned along the $[\bar{1}10]$ direction for the Si substrate, and the measured height (B) (SrF_2 film height) can be estimated to be about 0.15 nm in figure 1(c). In these topographic measurements, the bias voltage between the tip and sample was applied to compensate the contact potential difference between the Si tip and the area of the Si(111)-(7 × 7) surface. In the case of heterogeneous surfaces in NC-AFM, the Kelvin probe force microscopy method has been proposed for correct height measurements with active compensation of electrostatic forces [27]. Accordingly, the estimated value from this topography might be lower than the actual SrF_2 layer height. In addition, the structural model for the SrF_2 row structure is mandatory for the correct height measurement so far, whereas it has not been established by the other experimental techniques. Our topographic images in figures 2(a) and (c) have not been achieved with atomic resolution. Hence, experimental ingenuity to extract the source of atomic contrast is necessary for detailed analysis for the structural assumption of SrF_2 rows.

To scan the area of the SrF_2, the topography can be classified into two types of tip-dependent images. Figure 2 shows (a) the topographic and (b) the corresponding dissipative images of the same SrF_2 surface for 0.4 ML coverage. The topographic image in figure 2(a) was observed only with the particular tip that was used to simultaneously image both row structures of SrF_2 and the Si(111)-(7 × 7) surface (type I tip apex in the following). On the other hand, figure 2(c) was obtained when the tip was occasionally attached to the SrF_2 surface (type II tip apex in the following). Under scanning the Si(111)-(7 × 7) surface area with the type II tip, no image was obtained on the (7 × 7) surface; however, it changed to the type I tip apex by the tip crash process.

The Si(111)-(7×7) surface was clearly observed using the type I tip apex, allowing that the row structure was imaged over the step edge of SrF_2. The A and B rows in figures 2(a) and (b) aligned alternately, and the separation in each case was typically about 1.0 nm wide. On the other hand, rows C in figure 2(c) were also aligned with a periodicity of 1.0 nm. These images, however, were obtained for the same surface of SrF_2 and have quite different corrugations.

According to the insulating surfaces, the chemical interaction forces acting between the ionic atoms at the tip end and individual surface ions play an important role for obtaining NC-AFM images with atomic resolution [11, 28]. In this case, the type II tip was produced by type I tip scanning on the SrF_2 surface by incidental crashing, and it can be considered that the type II tip acts as a type I tip with ionic atoms at the tip end. Using the type II tip, furthermore, it was quite difficult to obtain an image of the Si(111)-(7 × 7) surface under typical experimental conditions.

On the other hand, imaging with the type I tip was achieved for the Si (111)-(7 × 7) surface with atomic resolution and was regarded as being due to reactive Si dangling bonds.

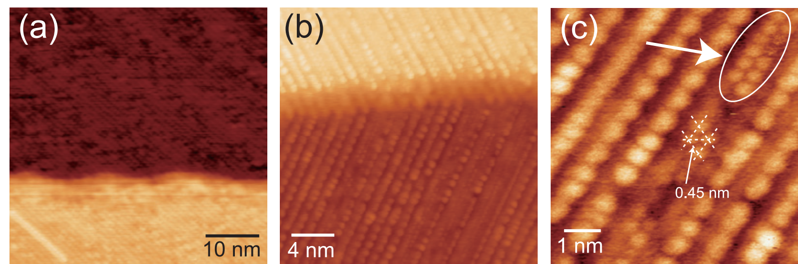

Figure 3. NC-AFM topographic images on the surface of $SrF_2/Si(111)$ for 0.7 ML SrF_2 coverage. The scanning sizes are (a) 48 × 48 nm^2, (b) 24 × 24 nm^2 and (c) 7 × 7 nm^2, respectively. The acquisition parameters were (a) $f_0 = 172\,202.8$ Hz, $A = 6$ nm, $\Delta f = -24.0$ Hz, (b) $f_0 = 181\,996.4$ Hz, $A = 5$ nm, $\Delta f = -23.2$ Hz, and (c) $f_0 = 181\,996.4$ Hz, $A = 5$ nm, $\Delta f = -26.6$ Hz, respectively.

The topographic image in figure 2(a) shows the row structure, not the (1 × 1) structure. This is different from the bulk periodicity, indicating that the bonding between the ionic constituents on this surface has the possibility to be weak for ionic bonding features. In addition, the proposed theoretical prediction indicates that using dangling-bond-terminated Si tips offers an opportunity for chemically resolved imaging of insulating surfaces with surface anions [26].

By the above considerations, the type I and II tip apexes have different characteristics for imaging the SrF_2 row structure. The former is estimated to be the reactive Si tip apex, whereas the latter is estimated to be the ionic tip apex.

During topographic NC-AFM measurements, as indicated below, the tip–sample contact potential difference was compensated by applying a corresponding bias voltage.

3.2. 0.7–1.2 *monolayer coverage of SrF_2 on Si(111)*

Figure 3 shows NC-AFM topographic images on the $SrF_2/Si(111)$ surface for SrF_2 coverage of 0.7 ML. As shown in figure 3(a), the corrugation of rows was observed over the whole area, and the image was classified as the type II tip apex. When the coverage was above 0.7 ML as shown by the arrow in the figure 3(c), the corrugation indicated that excess SrF_2 molecules partially filled the depression between the rows to be formed with (1 × 1) periodicity with concurrent conformation change of the row structure in the area surrounded by a circle in figure 3(c). The period of atomistic corrugation was estimated to be about 0.45 nm, and the value corresponded to about 10% expansion of the bulk length (0.41 nm). This expansion is attributed to lateral discommensuration with the Si substrate [18].

Figure 4 shows NC-AFM topographic images of the $SrF_2/Si(111)$ surface for 1.1 ML coverage of SrF_2. As shown in figure 4(a), the row structure near the centre of the terraces and the flat step edge with triangular shape were observed simultaneously. In the flat step edge, corrugation with (1 × 1) periodicity was also observed from the high resolution topographic image in figure 4(b). This indicates that the local areas of (1 × 1) periodicity spread from the edge to the centre of the terrace by further evaporation of SrF_2. Figure 4(c) corresponds to the cross-sectional line profile on the line shown in figure 4(b). The distance between the corrugations was, however, estimated to have the same value as the bulk. This indicates that the arrangement was affected by the substrate at the early stages of SrF_2 growth, and the (1 × 1) structure with expanded lattice constant was formed on the partial area accordingly. The (1 × 1) structure with the bulk value was, however, formed from the step edge by further SrF_2 evaporation.

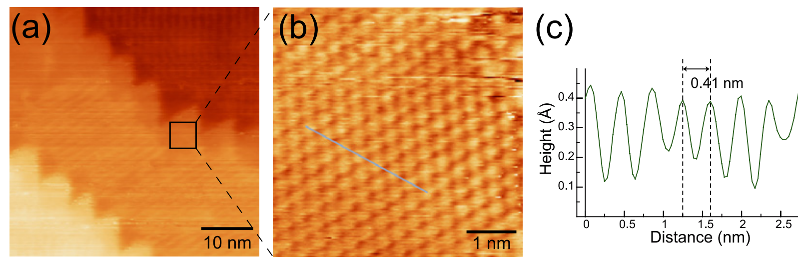

Figure 4. NC-AFM topographic images of the surface of $SrF_2/Si(111)$ for 1.1 ML SrF_2 coverage. Scanning size is (a) $48 \times 48\ nm^2$ and (b) $5 \times 5\ nm^2$, respectively. (c) The line profile corresponds to the solid line in (b). The acquisition parameters were (a) $f_0 = 175\,952.8$ Hz, $A = 6$ nm, $\Delta f = -19.0$ Hz, and (b) $f_0 = 175\,952.8$ Hz, $A = 6$ nm, $\Delta f = -27.5$ Hz, respectively.

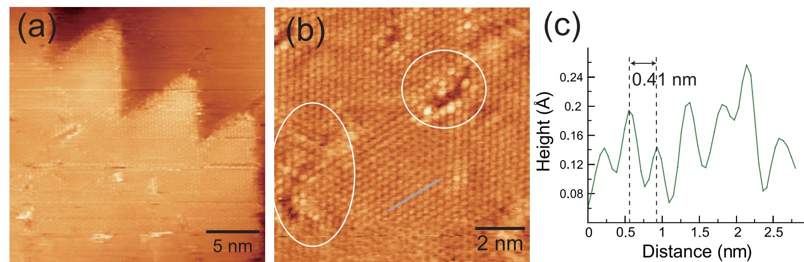

Figure 5. NC-AFM topographic images on the surface of $SrF_2/Si(111)$ for 1.2 ML SrF_2 coverage. Scanning sizes are (a) $24 \times 24\ nm^2$ and (b) $12 \times 12\ nm^2$, respectively. (c) The line profile corresponds to the solid line in (b). The acquisition parameters used were (a) $f_0 = 175\,953.9$ Hz, $A = 6$ nm, $\Delta f = -34.5$ Hz, and (b) $f_0 = 175\,952.8$ Hz, $A = 6$ nm, $\Delta f = -64.2$ Hz, respectively.

3.3. 1.2∼ *monolayer coverage of* SrF_2 *on Si(111)*

Figures 5(a) and (b) show NC-AFM topographic images of the $SrF_2/Si(111)$ surface for 2.2 ML SrF_2 coverage. The whole area was covered with a hexagonal arrangement with (1×1) periodicity, and the features are similar to the case of a 2 ML CaF_2 (111) surface grown on Si(111) [29]. The corrugation interval was estimated to have the same value as the bulk (0.41 nm) from the line profile in figure 5(c). On the other hand, domain boundaries, defects and long-period surface undulation were found in most parts of the SrF_2 surface shown in the area surrounded by circles in figure 5(b), indicating that they could be attributed to structural relaxation with (1×1) periodicity. An atomic resolution image obtained by the constant height mode, furthermore, showed that the line profile of the surface corrugation represents the same features in comparison with the results for the $CaF_2(111)$ surface with the negative termination tip [11, 29]. This indicates that the surface consists of the F–Sr–F triple layer and is very similar to the features of the bulk $SrF_2(111)$ surface.

4. Conclusions

We have imaged SrF_2 film surfaces on Si(111) using NC-AFM to explore the growth dynamics of the insulating film and to reveal the conformation changes due to the role of lattice mismatch between the SrF_2 and Si. These topographic images obtained in figures 1–5 provide features of the growth dynamics on the insulating SrF_2 film surface using NC-AFM as follows.

(i) For ∼0.7 monolayer (ML) SrF_2 coverage, the film surface formed row-like structures of SrF_2, which was quite different from the bulk, indicating that this represents surface

reconstruction due to the large lattice mismatch effect at the interface. In addition, we obtained two types of tip-apex-dependent NC-AFM topographic images. One, derived from the tip apex with Si dangling bonds, provides simultaneous imaging of both the SrF_2 row structure and the Si(111)-(7 × 7) surface. The corrugation of the rows could be considered to be fluorine constituents. The other, derived from the ionic tip apex, was considered to be a corrugation of strontium rows by the simple assumption of the structural configuration.

(ii) At around 0.7 ML SrF_2 coverage, the surface was formed into row structures, indicating that this represents the two-dimensional growth mode. With further ∼1.2 MLSrF_2 coverage, the surface conformation was partially changed from the row structure to expanded (1 × 1) periodicity in comparison to the bulk. The conformation change occurred from the step edge to the terrace, and the resulting developed area by further coverage indicated the (1 × 1) periodicity with the same value as the bulk.

(iii) At 1.2∼ MLSrF_2 coverage, the atomistic corrugation of the hexagonal arrangement was observed all around. In addition, we observed defects, domain boundaries and height undulation derived from lattice mismatch at the interface between SrF_2 and Si, allowing that the atomistic corrugation kept the (1 × 1) periodicity.

These results presented here clearly demonstrate that NC-AFM is a real-space observation technique that can determine the local atomistic structure, for growth dynamics of insulating films. With respect to the SrF_2/Si(111) surface with ∼0.7 ML coverage, further experimental investigations are necessary to obtain NC-AFM images with improved imaging stability, and theoretical simulations are needed for a clear understanding of the interface and surface structure. In addition, atom discrimination by force spectroscopy and kelvin probe force spectroscopy, which represents force spectroscopy with active compensation of electrostatic forces, could be applicable novel techniques for obtaining detailed structural depth information independent of the materials used.

Acknowledgments

This work has been supported by the 21st Century COE Programme (G18) of the Japan Society for the Promotion of Science and the Ministry of Education, Science, Sports and Culture, Grant-in-Aid for Young Scientists (B), 17710100, 2005–2006.

References

[1] Morita S, Wiesendanger R and Meyer E 2002 *Noncontact Atomic Force Microscopy* (Berlin: Springer)
[2] Giessibl F J 1995 *Science* **267** 68–71
[3] Kitamura S and Iwatsuki M 1995 *Japan. J. Appl. Phys.* **270** L145–148
[4] Sugawara Y, Ohta M, Ueyama H and Morita S 1995 *Science* **270** 1646–8
[5] Loppacher Ch, Bammerlin M, Guggisberg M, Schär S, Bennewitz R, Baratoff A, Meyer E and Güntherodt H-J 2000 *Phys. Rev.* B **62** 16944–9
[6] Barth C and Reichling M 2001 *Nature* **414** 54–7
[7] Bennewitz R, Schär S, Barwich V, Preiffer O, Meyer E, Krok F, Such B, Kolodzej J and Szymonski M 2001 *Surf. Sci.* **474** L197–202
[8] Bennewitz R, Foster A S, Kantorowich L N, Bammerlin M, Loppacher Ch, Schär S, Guggisberg M, Meyer E and Shluger A L 2000 *Phys. Rev.* B **62** 2074–84
[9] Burke S A, Mativetsky J M, Hoffmann R and Grütter P 2005 *Phys. Rev. Lett.* **94** 096102
[10] Kunstmann T, Schlarb A, Fendrich M, Wagner Th, Möller R and Hoffmann R 2005 *Phys. Rev.* B **71** 121403(R)
[11] Barth C, Foster A S, Reichling M and Shluger A L 2001 *J. Phys.: Condens. Matter* **13** 2061–79
[12] Foster A S, Gal A Y, Gale J D, Lee Y J, Nieminen R M and Shluger A L 2004 *Phys. Rev. Lett.* **92** 036101

[13] Schowalter L J and Fathauer R W 1989 *Crit. Rev. Solid State Mater. Sci.* **15** 367–421
[14] Ishiwara H and Asano T 1982 *Appl. Phys. Lett.* **40** 66–8
[15] Asano T and Ishiwara H 1983 *Appl. Phys. Lett.* **42** 517–9
[16] Satpathy S and Martin R M 1989 *Phys. Rev.* B **39** 8494–8
[17] Olmstead M A and Bringans R D 1990 *Phys. Rev.* B **41** 8420–30
[18] Denlinger J D, Olmstead M A and Rotenberg E 1991 *Phys. Rev.* B **43** 7335–8
[19] Rotenberg E, Denlinger J D, Leskovar M, Hessinger U and Olmstead M A 1994 *Phys. Rev.* B **50** 11052–69
[20] Albrecht T R, Grütter P, Horne D and Rugar D 1991 *J. Appl. Phys.* **69** 668–73
[21] Horcas I, Fernández R, Gómez-Rodríguez J M, Colchero J, Gómez-Herrero J and Baro A M 2007 *Rev. Sci. Instrum.* **78** 013705
[22] Nakayama T, Katayama M, Selva G and Aono M 1994 *Phys. Rev. Lett.* **72** 1718–21
[23] Nakayama T and Aono M 1998 *Phys. Rev.* B **57** 1855–9
[24] Sumiya T 2000 *Surf. Sci.* **156** 85–96
[25] Pfeiffer O, Gnecco E, Zimmerli L, Maier S, Meyer E, Nony L, Bennewitz R, Diederich F, Fang H and Bonifazi D 2005 *J. Phys. Conf. Ser.* **19** 166–74
[26] Foster A S, Gal A Y, Gale J D, Lee Y J, Nieminen R M and Shluger A L 2004 *Phys. Rev. Lett.* **92** 036101
[27] Sadewasser S and Lux-Steiner M Ch 2003 *Phys. Rev. Lett.* **91** 266101
[28] Hoffmann R, Barth C, Foster A S, Shluger A L, Hug H J, Güntherodt H-J, Nieminen R M and Reichling M 2005 *J. Am. Chem. Soc.* **127** 17863–6
[29] Seino Y, Abe M and Morita S 2005 *Mater. Res. Soc. Symp. Proc.* E **838** O1.9.1–6